

Measurements of ρR asymmetries at burn time in inertial-confinement-fusion capsules

F. H. Séguin, C. K. Li, J. A. Frenje, S. Kurebayashi, and R. D. Petrasso^{a)}

Plasma Science and Fusion Center, Massachusetts Institute of Technology, Cambridge, Massachusetts 02139

F. J. Marshall, D. D. Meyerhofer,^{b)} J. M. Soures, T. C. Sangster, C. Stoeckl, J. A. Delettrez, P. B. Radha, V. A. Smalyuk, and S. Roberts

Laboratory for Laser Energetics, University of Rochester, Rochester, New York 146211

(Received 5 March 2002; accepted 2 May 2002)

Recent spectroscopic analysis of charged particles generated by fusion reactions in direct-drive implosion experiments at the OMEGA laser facility [T. R. Boehly *et al.*, *Opt. Commun.* **133**, 495 (1997)] show the presence of low-mode-number asymmetries in compressed-capsule areal density (ρR) at the time of fusion burn. Experiments involved the acquisition and analysis of spectra of primary (14.7 MeV) protons, from capsules filled with deuterium and helium-3, and secondary (12.6–17.5 MeV) protons, from cryogenic deuterium capsules. The difference between the birth energy and measured energy of these protons provides a measure of the amount of material they passed through on their way out of a capsule, so measurements taken at different angles relative to a target provide information about angular variations in capsule areal density at burn time. Those variations have low-mode-number amplitudes as large as $\pm 50\%$ about the mean (which is typically ~ 65 mg/cm²); high-mode-number structure can lead to individual pathlengths through the shell that reach several times the mean. It was found that the observed ρR asymmetries are often similar for contiguous implosions, but change when the laser beam energy balance is significantly changed, indicating a direct connection between drive symmetry and implosion symmetry. © 2002 American Institute of Physics. [DOI: 10.1063/1.1492806]

I. INTRODUCTION

Achieving spherical symmetry in the assembled mass of inertial-confinement-fusion (ICF) capsule implosions is a critical prerequisite for optimal burn and ignition.¹ Numerical simulations are often used to predict the conditions under which asymmetries may develop,² but quantitative experimental information about asymmetries in total areal density (ρR) has been limited. Previous work has included x-ray measurements which provide information about asymmetries in capsule shells, but only within shell sublayers doped with Ti.³ In addition, spectra of low-energy charged particles from implosions of low- ρR capsules have been interpreted as including effects of ρR variations within limited areas on the shell (using alpha particles from glass microballoons filled with DT [deuterium–tritium],⁴ and DD protons from D₂-filled capsules⁵). Here we present the first absolute measurements of low-mode-number asymmetries in total capsule ρR at fusion burn time, from direct-drive implosions of thick-shelled capsules at the OMEGA⁶ laser facility. As proposed previously,⁷ this was accomplished by studying the slowing down of energetic protons whose birth spectrum is well characterized (in this case primary and secondary D³He protons) at many different angles around individual capsules.

Measured energy losses are related to the ρR through which protons pass on their way out of a capsule.^{8,9}

Possible sources of implosion asymmetry include exponentially-growing Rayleigh–Taylor (RT) instabilities and linearly growing secular modes, either of which can be seeded by small-amplitude asymmetries in either initial capsule structure or laser irradiation. The OMEGA facility utilizes 60 laser beams, and the shapes and overlaps of the individual beams are designed to minimize the total rms nonuniformity of power deposition. Nonuniformities within individual beams can generate perturbations with high-mode numbers ($l > 10$), and recent work has resulted in beam smoothing methods (1 THz smoothing by spectral dispersion with polarization smoothing¹⁰) that reduced single-beam nonuniformities. These reduced nonuniformities have resulted in better capsule implosion characteristics,^{9,11,12} presumably as a consequence of reduced RT seeding and a resulting reduction in fuel–shell mix.^{12,13}

Imbalances in the on-target power deposition of separate beams can result in low-mode-number ($l < 10$) perturbations, driving secular modes which are the focus of this paper. There are currently two methods of adjusting the beam balance at OMEGA. The “standard” method involves measurement of the energy in each beam just after conversion of laser light from infrared (IR) to ultraviolet (UV), and prediction of actual on-target power on the basis of the measured efficiency of light transmission to the target location; the individual beams are then adjusted to produce the best predicted on-target power balance. A new method, referred to as

^{a)}Also visiting Senior Scientist, Laboratory for Laser Energetics, University of Rochester.

^{b)}Also at Departments of Mechanical Engineering and Physics, and Astronomy, University of Rochester.

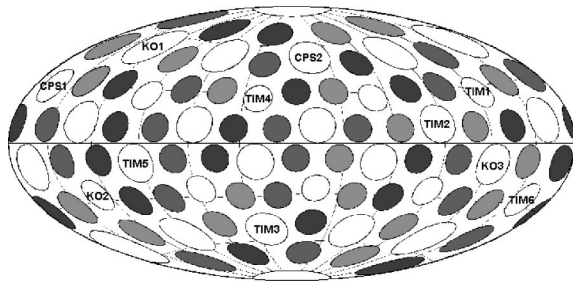


FIG. 1. Locations of diagnostic ports on the OMEGA target chamber, shown on an Aitoff projection. The positions labeled CPS1 and CPS2 correspond to permanently mounted, magnet-based spectrometers. The other labeled ports can sometimes be used for wedge-range-filter proton spectrometers.

the “x-ray” method,¹⁴ attempts to make measurements that directly determine the relative on-target energy in different beams by imaging x-ray emission from a special target (4 mm in diameter and coated with Au) when illuminated by the laser. Individual IR amplifier gains are then adjusted to balance the x-ray power generated by the individual beams.

The charged-particle measurements described here demonstrate that easily measurable changes in ρR asymmetry are sensitive to changes in the beam balance. The nature of the measurements, and their relationship to capsule asymmetries, is discussed in Sec. II. Proton spectra from D–³He-filled capsules with thick plastic (CH) shells frequently demonstrate asymmetries in both yield and energy, and these are discussed separately. Asymmetries in proton yield have some interesting properties, but are discussed only in the Appendix because there is strong evidence that they are not directly correlated with capsule structure. Asymmetries in proton energy, discussed in Sec. III, are interpreted as unique signatures of capsule areal density asymmetries; they are shown to be correlated with differences in laser beam balance. Preliminary data involving secondary protons from cryogenic D₂ capsules are also shown. Finally, a brief comment on the information content of individual proton spectra is presented in Sec. IV.

II. CHARGED-PARTICLE MEASUREMENTS AND CAPSULE STRUCTURE

A. Measured particle energy and capsule ρR

Up to 11 diagnostic port locations can now be used for charged-particle spectrometry on the OMEGA target chamber, as illustrated in Fig. 1. Two magnet-based spectrometers,

CPS1 and CPS2,^{15,16} are permanently mounted on two of the ports, while “wedge-range-filter” spectrometers (WRFs)¹⁶ can be mounted on the other ports.

Symmetry data have been collected for a variety of capsule types, utilizing protons in the 15 MeV energy range that are generated by the reactions listed in Table I. These protons are of far more general use than either higher-*Z* fusion products (e.g., 3.5 MeV DT α) or lower-energy (e.g., 3 MeV DD) protons, since they can escape compressed capsules with much higher values of total (fuel plus shell) areal density (up to at least 200 mg/cm²). The protons have known birth spectra, and as they pass out of a capsule they lose energy in proportion to the amount of material they pass through (ρR_{total}). A value of ρR_{total} for the portion of a capsule facing a given spectrometer can be estimated⁸ from the downshift in mean proton energy $\Delta(Ep)$ by using an appropriate theoretical formulation for the slowing down of protons in a plasma¹⁷ (this estimate is insensitive to uncertainties in the temperature and density of the shell, which accounts for the majority of the energy loss^{8,9,16}).

To justify the association between energy asymmetries and capsule structure asymmetries it is necessary to explain why an observed energy asymmetry cannot be a result of uneven modification of proton energies by electric fields outside the capsule. This is an important issue, because it is known that target capsules become charged to a significant electric potential (~ 0.5 – 1 MV) during laser exposure due to laser–shell interactions;^{8,18} when the capsule “burn time” occurs during the laser pulse (as it can when a capsule shell is thin), the result is that charged particles are accelerated to higher energy while traveling between capsule and detector.⁸ This electric potential dissipates quickly after the laser pulse, however. When the capsule burn occurs a few hundred ps after the laser pulse ends, as it does for the type of capsule studied here, the radial electric field is essentially gone and the measured energies of particles reflects their actual values after leaving the capsule. This was demonstrated directly by measurements of knock-on protons from implosions of DT-filled capsules with shells, fill pressures, and laser conditions comparable to those under study here.¹¹ The knock-on protons are from the CH shell, elastically scattered by 14.1 MeV DT neutrons from the fuel. Because some of the protons are scattered at the outer surface of the shell and will not slow down due to interactions with the capsule, the high-energy limit of the proton spectrum at the capsule surface should always be 14.1 MeV. When this spectrum is measured at different angles during each of many shots, using WRFs, the high-energy limit is always 14.1 MeV to within statistical

TABLE I. Reactions producing protons in the 15 MeV energy range in capsules used at OMEGA.

Fuel	Proton source	
D– ³ He	D + ³ He → α [3.6 MeV]	+ p [14.7 MeV]
D ₂	D + D → n [2.45 MeV] + ³ He[0.82 MeV], ³ He[\leq 0.82 MeV] + D → α [6.6–1.7 MeV]	+ p [12.6–17.5 MeV]
D–T ^a or D–T–H	D + T → α [3.5 MeV] + n [14.1 MeV], n [14.1 MeV] + p → n'	+ p [\leq 14.1 MeV]

^aWith D–T fuel, knock-on protons are produced only if the shell contains H.

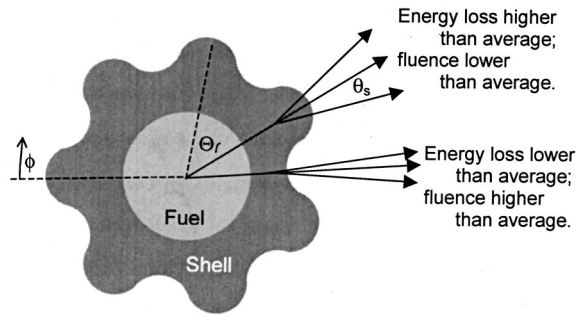


FIG. 2. Schematic illustration of how angular variations in capsule ρR might generate angular variations in the energies and fluences of protons that were produced at the center of the fuel (in the artificial “hot-spot” model) but detected outside the capsule. If ϕ is an angle in this cross section, structure with the form $\rho R(\phi) = \rho R_0[1 + A \cos(l\phi)]$ would result in an angle $\Theta_l = l/2\pi$ between ρR maxima. As protons pass through the shell at angle ϕ , they lose energy $\Delta E(\phi) \propto \rho R(\phi)$. They also spread slightly in angle by an amount $\theta_s(\phi) \propto \rho R(\phi)$, since energy loss is due primarily to small-angle scattering. A small detector at a distance much greater than the capsule radius would intercept protons from an angular region in the capsule with size $\delta\phi \sim 2\theta_s$, and this fact determines what types of angular variations would be seen by a group of such detectors at different ϕ . The result depends on how Θ_l compares with $2\theta_s$ or, equivalently, how l compares with π/θ_s , as will be demonstrated in the numerical simulations shown in Fig. 3 and as discussed in a footnote (Ref. 19). For values of l that are small (compared to π/θ_s), angular variations in ΔE are detectable but no angular variations in fluence could be seen. For $l \sim \pi/\theta_s$, angular variations in both ΔE and fluence could be seen. For large enough l , no variations could be measured for either ΔE or fluence.

and calibration uncertainties,¹¹ indicating that no acceleration occurs between shell and detector.

B. Sensitivity of the measurements to capsule structures with different mode numbers

Figure 2 illustrates how capsule asymmetries could result in asymmetries in proton energies and yields, in the artificial situation in which all protons are created in an infinitesimal volume at the center of the fuel (a “hot-spot” model). The protons should be produced with spherically symmetric distributions of energy and yield, even if the fuel itself is asymmetric. Passage through a shell with angular ρR variations results in an angular variation in mean proton energy, since energy loss is roughly proportional to ρR . In principle, there would also be an asymmetry in the yield (where by yield we mean the inferred total particle yield as inferred from the fluence at a given angle). This is because the slowing down of protons, as they pass through the capsule material, occurs primarily through small-angle scattering off electrons, so the protons that started in a particular direction will be spread over a small angle θ_s after passage through the shell. The size of θ_s is roughly proportional to the amount of slowing down. The result, as discussed in the caption of Fig. 2, is that there should be a negative change in yield at observation angles that correspond to larger ρR and larger energy downshift. At small mode numbers, where the angle between ρR maxima is much greater than θ_s , yield variations should not be measurable but energy variations should be detectable. Neither yield nor energy variations should be detectable when the mode number is large enough

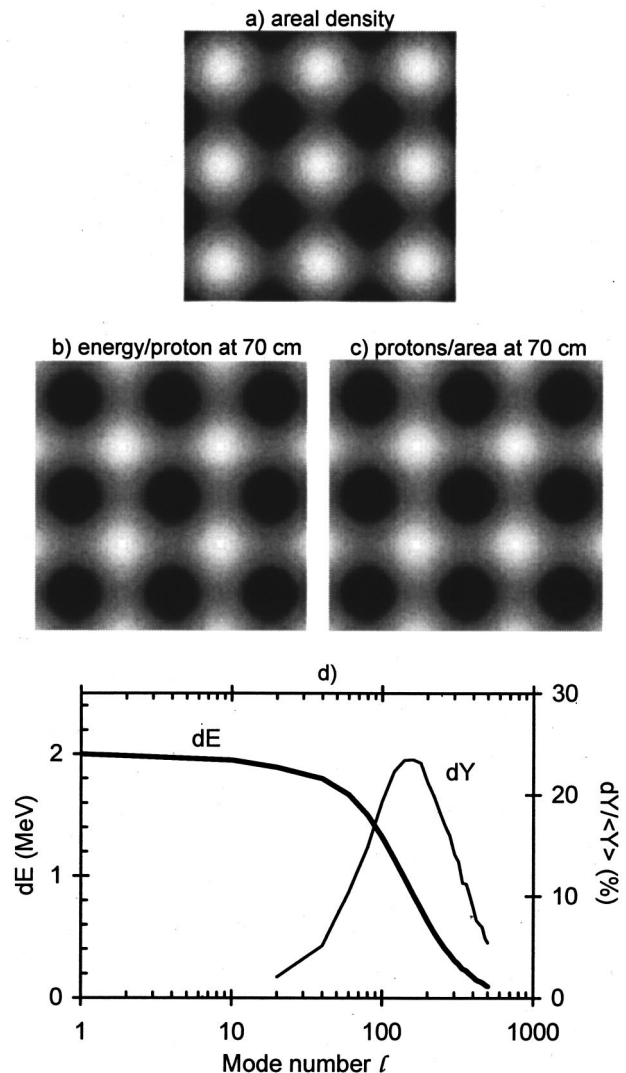


FIG. 3. Numerical simulation to demonstrate the principle described in the previous figure. 14.7 MeV protons were assumed to originate at the center of a capsule (“hot-spot” model), and to pass through a 20 g/cc, 1 keV CH shell with an average areal density of 60 mg/cm². The areal density of the shell was assumed perturbed by a two-dimensional, sinusoidal structure with mode number l , and amplitude 30 mg/cm² (so the minimum value was 30 mg/cm² and the maximum was 90 mg/cm²), as illustrated in the grayscale image labeled (a), where brightness is proportional to areal density and black is mapped to the minimum value. At a distance of 70 cm from the capsule, the mean energy and fluence of protons was calculated in a “detector” plane normal to the capsule-detector direction. The results are illustrated in the images labeled (b) and (c), where brightness is proportional to energy per proton and protons per unit area, respectively (with black mapped to the minimum value in each case); the area represented covers the same solid angle, as seen from the center of the capsule, as that shown in (a). The peak-to-peak amplitudes of the energy and fluence/area calculations, as a function of mode number, are shown in (d). Energy loss in the CH plasma was calculated according to Ref. 17, while estimates for the scattering angles of protons were obtained with the Monte Carlo program TRIM (Ref. 20). (TRIM applies to cold matter, rather than a plasma, but there is little difference for the small-angle scattering of the 14.7 MeV protons since their energies greatly exceed both the thermal energies of the shell plasma electrons [~ 0.5 –1 keV] and the binding energies of electrons in atomic C or H [< 0.3 keV].)

so that the angle between ρR maxima is smaller than θ_s . These effects are illustrated in Fig. 3, which shows numerical simulations for a particular capsule configuration.

In reality, the source of protons will be distributed over a

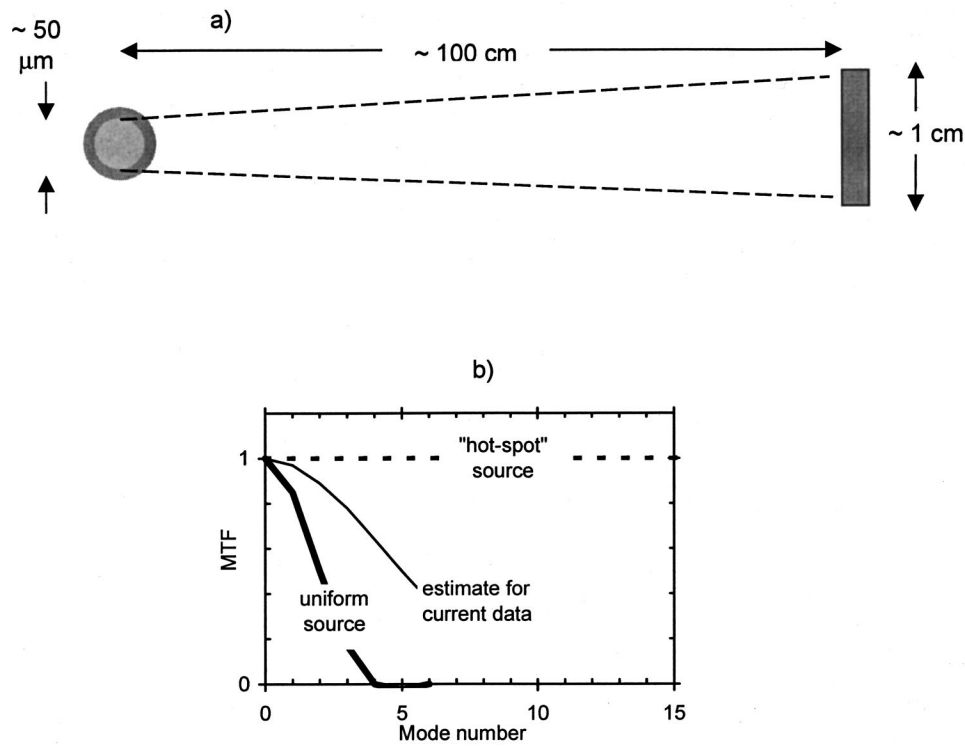


FIG. 4. (a) Relationship between a target capsule (left) and the active area of a spectrometer (right). In this simplified cartoon, the capsule is shown as consisting of fuel contained in a well-defined shell. If particle production extends throughout the fuel volume, detected particles will sample a substantial fraction of the capsule surface. (b) The modulation transfer function, or detectability of structure with different mode numbers, for different assumptions about the size of the region in the fuel where particle production occurs. In the artificial “hot-spot” scenario described in Figs. 2 and 3, with the source of particles localized at the center of the fuel, any mode could be detected. In the opposite extreme, where particle production occurs uniformly throughout the fuel volume and the shell is infinitely thin, each measurement averages over a sufficiently large fraction of the capsule that only mode numbers less than ~ 4 would be detectable. An intermediate situation would result in an intermediate MTF, and it can be shown from the information content in data sets described in this paper that the middle curve may approximate the response obtained here.

substantial volume of the fuel, so any external spectrometer measurement will include protons sampling a significant fraction of the capsule surface. Neither yield variations nor energy variations should be measurable when the size of the source exceeds the spacing between ρR maxima. Figure 4 illustrates the measurement geometry and the resultant sensitivity to mode structure; we are likely to be sensitive only to mode numbers under 10 when we look for angular variations in mean proton energy (although the presence of

higher-mode structure could manifest itself within the structure of individual spectra, as discussed below in Sec. IV).

In conclusion, the measurement techniques described here should be sensitive to ρR -induced angular variations in mean proton energy only for small mode numbers. The techniques should not be sensitive to any angular variations in yield that are due to capsule structure, since they would occur at mode numbers well above our sensitivity threshold. The filtering out of higher mode numbers actually has a

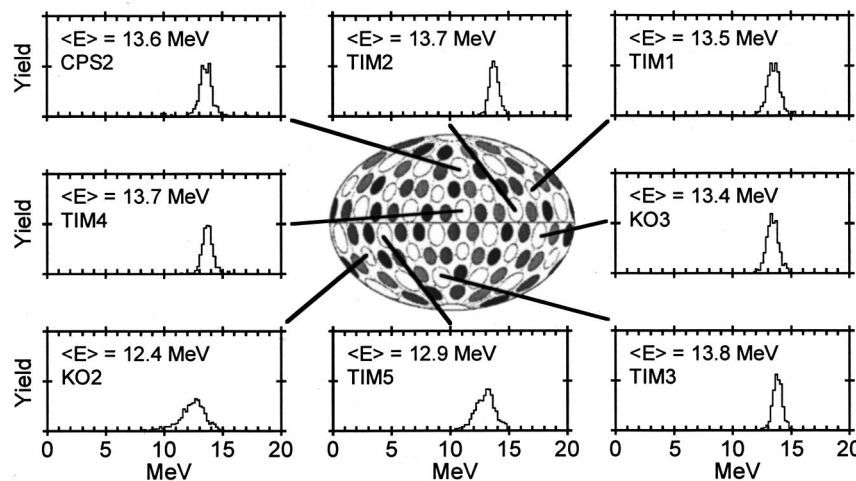


FIG. 5. Proton spectra measured simultaneously at eight different port positions during OMEGA implosion 21 240 (15 atm of $D-^3He$ fuel in a 20 μm thick CH shell, illuminated by 23 kJ of laser energy in 60 beams with a 1 ns flat-top pulse). The mean energy of each spectrum is listed here, and plotted in Fig. 6. The energies are all similar to one another, except for those measured at ports KO2 and TIM3, which were substantially lower.

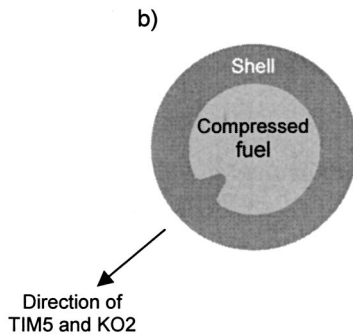
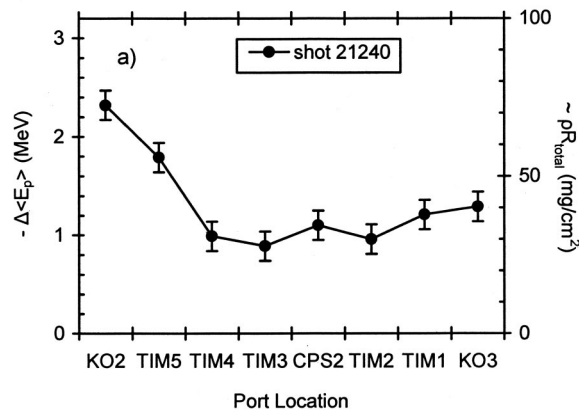


FIG. 6. (a) Mean change in energy plotted vs measurement port for the spectra illustrated in the previous figure. The right-hand vertical scale provides an estimate of the corresponding value of the total areal density ($\langle \rho R_{\text{total}} \rangle$). This was calculated using the slowing-down formalism of Ref. 17 together with the knowledge that most of the slowing down occurs in the shell (Refs. 8, 9, and 11) and the assumptions that the shell has a density of $\sim 20 \text{ g/cm}^3$ and a temperature of 0.5 keV [the result is very insensitive to uncertainties in these specific values (Refs. 8 and 16)]. Except for KO2 and TIM5, most of the energy losses are within experimental errors of each other. (b) Since KO2 and TIM5 are adjacent to each other, and since the spectra from the other six measurement directions sample most of the rest of the capsule surface, the simplest model of capsule structure would involve spherical symmetry except for a localized feature with higher ρR pointing in the direction of KO2 and TIM5. This simple cartoon illustrates a possible configuration, which is not claimed to be unique; in particular, the “bump” could protrude out of the shell rather than into the fuel.

beneficial effect. Since the current maximum number of spectrometers is only 11, any efforts to perform a modal decomposition or other complete analysis of capsule structure are limited to fairly simple structures (such as that illustrated in Fig. 6). The absence of sensitivity to high-mode numbers minimizes the likelihood of aliasing in the data from such modes.

III. ENERGY ASYMMETRIES, CAPSULE ASYMMETRIES, AND LASER BEAM BALANCE

Substantial energy asymmetries are often seen in the spectra of 14.7 MeV protons from thick-shelled D- ^3He -filled capsules. Figure 5 illustrates a sample set of eight spectra from a single implosion involving a capsule with a $20 \mu\text{m}$ CH shell and utilizing the standard beam-balance method. The energy downshifts of the spectra, relative to the birth energy of 14.7 MeV, are plotted in Fig. 6(a).

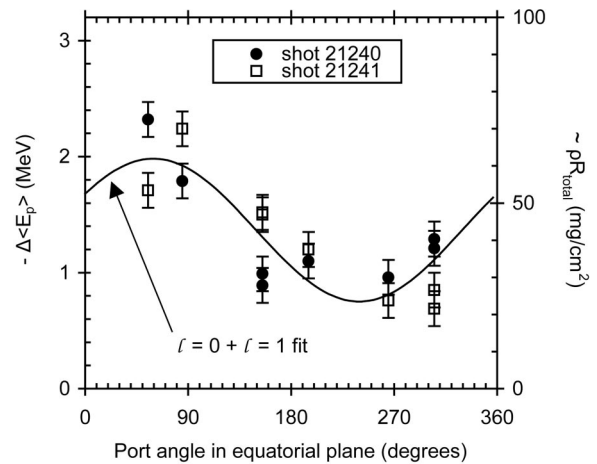


FIG. 7. Comparison of measured energy shifts for implosions 21 240 and 21 241, which were nominally identical. Note that the data points are plotted against longitudinal angle, but that the measurement positions were sometimes above, and sometimes below, the equator. While not identical, the results for the two implosions are similar. On-target, rms beam-to-beam energy nonuniformities were inferred, from UV intensity measurements, to be 2.5% for shot 21 240 and 3.0% for shot 21 241. The angular variations in energy shift suggest an $l=1$ mode.

Six of the eight downshifts are equal to one another within the measurement uncertainty, while the other two are larger by a factor of 2 and by several standard deviations. The two large downshifts were measured at ports KO2 and TIM5, which are adjacent to each other and near the equatorial plane of the chamber. The other six measurement locations provide views from 60 degrees above the equator, 60 degrees below the equator, and several angles around the equator. Figure 6(b) shows a possible (not necessarily unique) capsule structure that could generate such a data set.

Asymmetries in proton energies are often similar from one implosion to the next, as demonstrated in Fig. 7 where the downshifts are plotted as a function of longitudinal angle (although the ports are not all quite on the equator). The overall form of the data from shots 21 240 and 21 241 suggest that the dominant structure has a mode number of $l=1$ in longitudinal angle, although there are not enough measurements to rule out the possibility of aliasing in the data from higher modes.

More examples of implosion asymmetries are shown in Fig. 8, which also illustrates the relationship between capsule asymmetries and laser beam energy balance. Three sequences of contiguous implosions all involved capsules with D- ^3He fuel in $20 \mu\text{m}$ -thick CH shells, but the beam balance adjustment was different for each sequence. Within each sequence there is a strong similarity between energy shifts from implosion to implosion, indicating a basic repeatability. Between sequences there are significant differences in energy shifts, indicating changes in capsule symmetry with changes in laser beam balance.

Before the implosions illustrated in Fig. 8(a), the laser beams were balanced with the standard method. In spite of the fact that the two capsules had significantly different fill pressures (8 and 18 atm), the deviations from spherical symmetry are very similar (and the shot-to-shot similarity of ab-

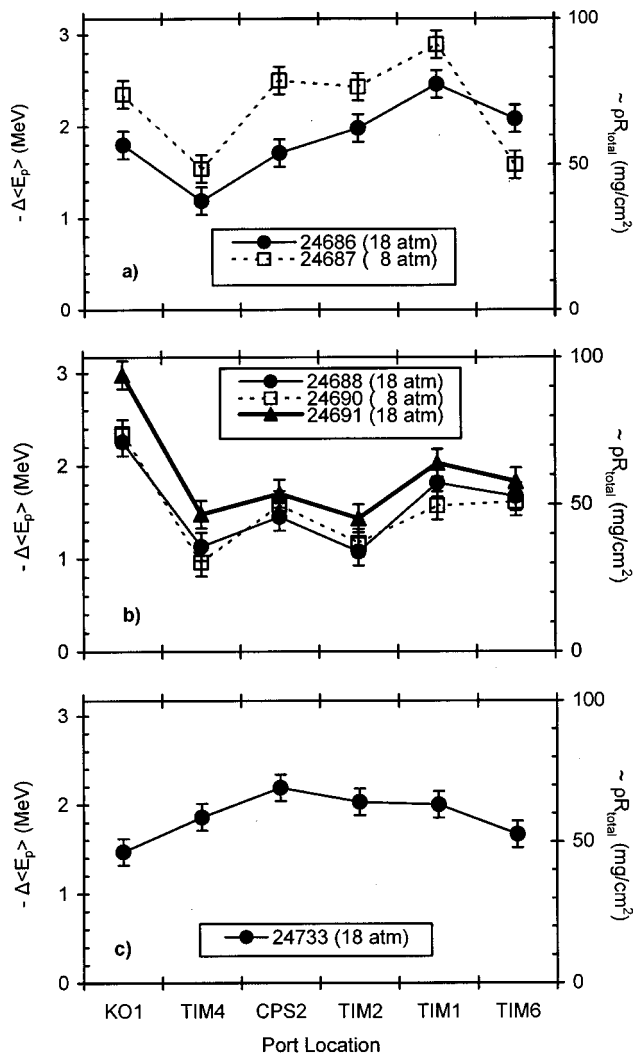


FIG. 8. Proton energy shifts measured at different port locations for three sequences of OMEGA implosions involving $D-^3He$ fuel in $20\ \mu m$ CH shells (all irradiated with 22 kJ of laser energy in 60 beams with 1 ns flat-top pulses). Each plot corresponds to a different laser balance adjustment, as discussed in the text, and each capsule had the fill pressure indicated. In this case it is not convenient to plot the measurements as a function of any single angle on the target chamber, because they do not lie near any great circle. On-target, rms beam-to-beam energy nonuniformities, inferred from UV intensity measurements, were 2.7% and 2.6% in the first sequence, 4.7%, 6.2%, and 6.2% in the second sequence, and 5.0% in the last shot.

solute ρR values is an example of how capsule compression is not very sensitive to fill pressure, in contrast to theoretical predictions, as discussed in Ref. 13). For each of these implosions, variations about the mean for on-target energy in the different laser beams was estimated with the standard balance method to be about 2.6% rms. However, the x-ray measurements performed for the x-ray balance method indicated a level of beam-to-beam nonuniformity of about 6.5% rms. Corrections for individual beams were made accordingly, with individual amplifier gains changed by as much as +13% and -12%. The three implosions represented in Fig. 8(b) represent those conditions; the angular ρR variations are remarkably similar to one another but quite different from those in Fig. 8(a). The level of beam-to-beam nonuniformity within each shot was estimated, from the x-ray balance mea-

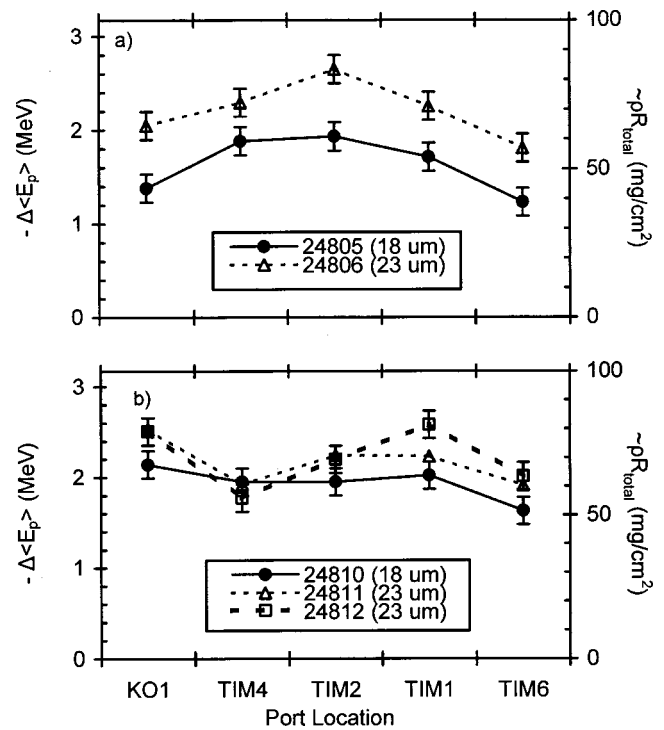


FIG. 9. Proton energy shifts measured at different port locations for two sequences of OMEGA implosions involving 18 atm of $D-^3He$ fuel in CH shells (all irradiated with 23 kJ of laser energy in 60 beams with 1 ns flat-top pulses). Each plot corresponds to a different laser balance adjustment, as discussed in the text, and each capsule had the shell thickness indicated. On-target, rms beam-to-beam energy nonuniformities, inferred from UV intensity measurements, were 2.8% and 2.9% in the first sequence, and 5.8%, 5.5%, and 5.5% in the second sequence.

surements, to be in the vicinity of 2% rms (while UV measurements indicated apparent nonuniformities of about 6%). The single implosion shown in Fig. 8(c) occurred after another iteration in the x-ray balance adjustment and shows somewhat better uniformity than seen in Figs. 8(a) or 8(b).

Figure 9(a) shows another group of two implosions following standard beam balance. Both capsules contained 18 atm of $D-^3He$, but the shell thicknesses were 18 and 23 μm , respectively. In spite of the difference in shells, the two implosions resulted in similar distortions from spherical symmetry although the thicker initial shell resulted in a higher ρR at burn time. Figure 9(b) shows a similar set of implosions after readjustment of the laser beam balance with the x-ray method. Once again, a change in beam balance changed the angular variations in measured ρR .

While the energy downshift data tend to be similar within a group of contiguous implosions with the same capsule characteristics and beam balance adjustments, there are some differences within each group. This would be expected even if the effects of beam balance are constant, since there are presumably other, and possibly random, seed perturbations such as defects in initial capsule shell uniformity.

Similar low-mode asymmetries are seen with secondary protons from D_2 -filled capsules. Preliminary data from room-temperature capsules is presented in Ref. 9, while a sample of results from preliminary work with cryogenic D_2

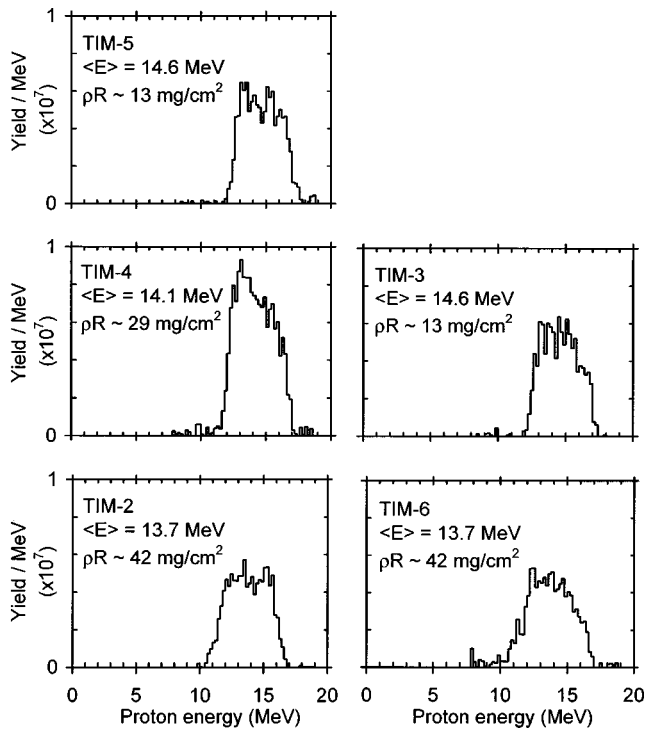


FIG. 10. Five spectra of secondary protons measured simultaneously during OMEGA implosion 24 096, with a cryogenic D_2 -filled capsule. The capsule had an outer diameter of $930 \mu\text{m}$, a $100 \mu\text{m}$ thick layer of D_2 ice inside a $1 \mu\text{m}$ CH shell, and a fill of D_2 gas (Ref. 21). It was irradiated by 24 kJ of laser energy in 60 beams, with a 1 ns flat-top pulse. On-target RMS beam-to-beam energy nonuniformity, inferred from UV intensity measurements, was 2.5%.

capsules is shown in Figs. 10 and 11 (see Ref. 21 for an overview of the cryogenic experiments at OMEGA).

IV. A NOTE ON THE STRUCTURES OF INDIVIDUAL SPECTRA

In our discussion of low-mode-number capsule structure we made use only of the mean energy of each spectrum, but (as mentioned in Sec. II B) the shapes of individual spectra

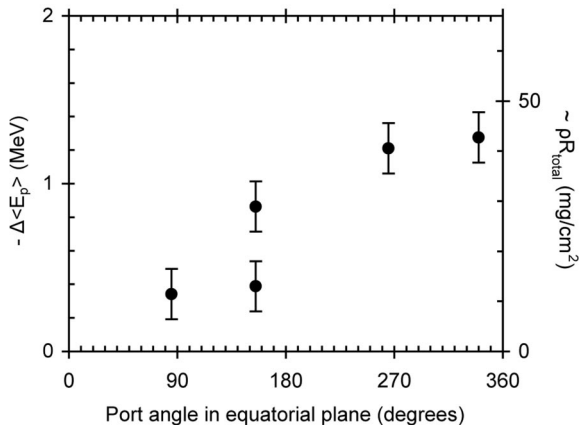


FIG. 11. The mean energy losses for five proton spectra shown in the previous figure. Although the diagnostic ports in this case did not all lie near a great circle on the target chamber, the energies have been plotted against the longitudinal angle. The two data points at about 150 degrees were measured above and below the equator, respectively.

can contain additional information. The total width of a spectral line is affected by instrument response, thermal broadening of particle birth energies, different pathlengths through fuel and shell for individual particles,^{4,5,8,16} and time evolution during burn.^{8,22} The spectra shown in Fig. 5 are examples of how individual widths can vary substantially. All spectra have nearly the same high-energy limit, because of a small component that is not very downshifted; this is generated by a transient shock coalescence²² when the shell is not completely compressed (and ρR_{total} is small), several hundred ps before the main burn. The different low-energy limits represent different maximum pathlengths. These maxima vary in Fig. 5 from $\sim 60 \text{ mg/cm}^2$ (for most of the ports) to $\sim 150 \text{ mg/cm}^2$ (for port KO2). That variation is qualitatively consistent with the cartoon of capsule structure shown in Fig. 6, which would result in a small number of pathlengths that are much longer than average and affect only spectrometers in one direction.

V. CONCLUSIONS

Spectrometry of charged fusion products provides unique information about low-mode-number deviations from spherical symmetry in imploded target capsules. The work reported here represents the first multiple-view measurements of absolute ρR_{total} values. Data from room-temperature $D-^3\text{He}$ fuel in CH shells indicate that changes in observed asymmetries are correlated with significant changes in laser beam balance, and that for a given beam balance they are often repeatable within contiguous groups of shots and relatively insensitive to differences in fuel fill pressure (8–18 atm) or shell thickness (18–23 μm). It is possible that the small variations that are seen within a group of implosions that are nominally identical are due to a more random source of perturbation, such as nonuniformities in the initial shell. Future experiments are planned for further investigation of all these phenomena with a wider variety of capsule types at OMEGA. Of particular interest will be experiments designed to introduce large, controlled amounts of laser beam imbalance in order to observe asymmetries in ρR and relate them to changes in implosion performance, and more experiments for determining whether the x-ray balance method results in improvements in implosion characteristics.

ACKNOWLEDGMENTS

This work was performed in part at the LLE National Laser Users' Facility (NLUF), and was supported in part by the U.S. Department of Energy Contract No. DE-FG03-99SF21782, LLE subcontract No. PO410025G, LLNL subcontract No. B313975, the U.S. Department of Energy Office of Inertial Confinement Fusion under Cooperative Agreement No. DE-FC03-92SF19460, and the New York State Energy Research and Development Authority.

APPENDIX: YIELD ASYMMETRIES

As discussed in Sec. II, the types of measurements used here should not detect proton yield asymmetries due to capsule structure under practical circumstances. In spite of that

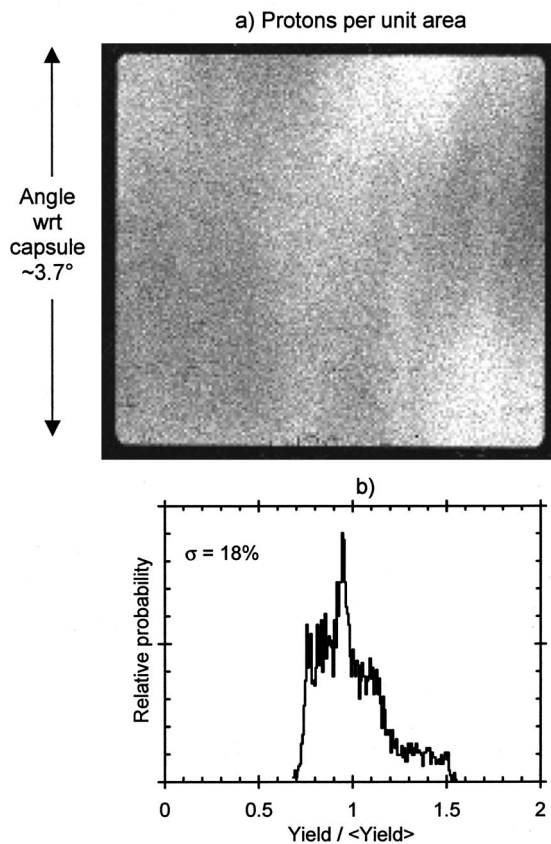


FIG. 12. (a) Spatial distribution of proton fluence as measured with a large-area CR-39 detector (5×7.5 cm), and displayed as a grayscale image, for OMEGA implosion 17 156 (15 atm of $D-^3He$ fuel in a $20 \mu m$ thick CH shell, illuminated by 24 kJ of laser energy in 60 beams with a 1 ns flat-top pulse). The CR39 detector faced the target at a distance of 70 cm, subtending an angle of about 3.7° from the target. The number of protons per unit area is proportional to brightness; the black border was covered by a thick aluminum frame, and had no protons. The rest of the area was covered by a uniform, $900 \mu m$ thick Al filter. Each pixel in the image corresponds to a physical area 0.125 mm^2 in area. (b) The probability distribution of fluence, or yield, relative to the average value, for all positions within the detector area (averaged over 0.12 cm^2 to reduce the effect of counting statistics).

fact, proton yield asymmetries are often observed (in a wide range of data including that discussed here and also secondary-proton yield data reported previously for implosions of room-temperature, D_2 -filled capsules^{23,9}). When multiple spectra are available for an individual shot, the yields typically have variations with standard deviations about the mean of 15%–20%; these variations are generally uncorrelated with energy variations and uncorrelated from shot to shot. Figures 12 and 13 show data from a special experiment in which the lack of correlation with energy is demonstrated in a straightforward way for the implosion of a $D-^3He$ -filled capsule with a $20 \mu m$ CH shell. The detector in this case was not a spectrometer, but a large-area sheet of CR-39 nuclear track detector that faced the capsule through an aluminum filter designed to range down the protons to energies within the CR-39 sensitivity range (about 0.2–8 MeV¹⁶). Figure 12(a) illustrates the number of particles per unit area incident on the detector at different positions, expressed as a grayscale image in which brightness is proportional to number density. Figure 12(b) shows the correspond-

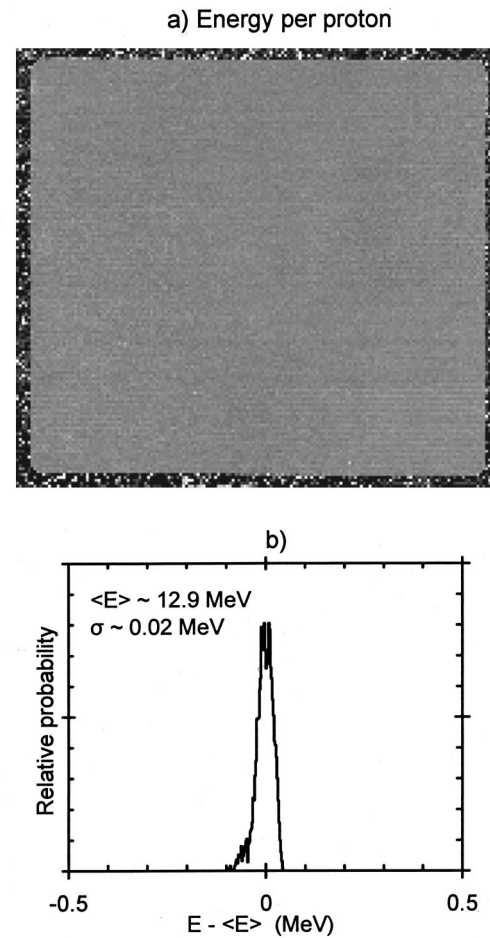


FIG. 13. (a) For the same data set illustrated in the previous figure, this grayscale image displays information about the spatial distribution of energy per proton. (b) Estimated probability distribution of the proton energy, for all positions within the detector (E is the energy at a given position, averaged over 0.12 cm^2 , and $\langle E \rangle$ is the energy averaged over the entire detector area). While the proton fluence over the detector area varies by a factor of 2, there is virtually no energy variation.

ing probability distribution of proton fluence values. There is a large variation in fluence seen here, with a maximum-to-minimum ratio of ~ 2 and a standard deviation of $\sim 18\%$ about the mean. The angular separation of the two fluence maxima of Fig. 12(a), measured with respect to the target capsule, is less than four degrees. If this were a projection of a structural aspect of the capsule, it would represent a mode number of order $l=100$. In view of our prediction that we should not be sensitive to mode numbers greater than ~ 10 , the yield variation should not be related to structure in the capsule.

Another reason for reaching the same conclusion is shown in Fig. 13(a), which illustrates a different aspect of the same data set. In this grayscale image, brightness is proportional to a measure of the mean energy per particle at a given location (protons generate circular tracks in the CR39 with diameters that correspond to their energies¹⁶). There is no obvious variation over the entire active detector area in spite of the large fluence variation. Figure 13(b) shows a probability distribution of mean energy per particle (estimated from the distribution of track diameters); it is extremely narrow

(<~0.1 MeV). From the discussion in Sec. II, we would have expected a large correlated energy perturbation if the yield perturbation were connected with capsule structure.

These two independent reasons imply that the yield variation is not caused by capsule structure. Since the protons should have been produced isotropically, it seems that something changed their directions slightly without changing their energies to a measurable extent. Two possibilities (un-corroborated so far by direct evidence) are magnetic fields²⁴ or small azimuthal electric fields outside the capsule. The amount of deflection from a radial trajectory required to re-organize the protons is about two degrees at the position of the detector, 70 cm from the target. This could be accomplished by a magnetic field of ~0.5 kG acting over the whole distance, or a larger field acting over a portion of the distance. Alternatively, electric field of ~25 kV/cm, perpendicular to the radial direction from the capsule over the target-detector distance, could generate a similar result.

¹S. W. Haan, S. M. Pollaine, J. D. Lindl *et al.*, Phys. Plasmas **2**, 2480 (1995).

²J. D. Lindl, *Inertial Confinement Fusion* (Springer-Verlag, New York, 1999).

³B. Yaakobi, V. A. Smalyuk, J. A. Delettrez, F. J. Marshall, D. D. Meyerhofer, and W. Seka, Phys. Plasmas **7**, 3227 (2000); V. A. Smalyuk, B. Yaakobi, J. A. Delettrez, F. J. Marshall, and D. D. Meyerhofer, *ibid.* **8**, 2872 (2001); V. A. Smalyuk, V. N. Goncharov, J. A. Delettrez, F. J. Marshall, D. D. Meyerhofer, S. P. Regan, and B. Yaakobi, Phys. Rev. Lett. **87**, 155002 (2001).

⁴A. P. Fews, M. J. Lamb, and M. Savage, Opt. Commun. **98**, 159 (1993).

⁵Y. Kitagawa, K. A. Tanaka, M. Nakai *et al.*, Phys. Rev. Lett. **75**, 3130 (1995).

⁶T. R. Boehly, D. L. Brown, R. S. Craxton *et al.*, Opt. Commun. **133**, 496 (1997).

⁷R. D. Petrasso, C. K. Li, M. D. Cable *et al.*, Phys. Rev. Lett. **77**, 2718 (1996).

⁸C. K. Li, D. G. Hicks, F. H. Séguin *et al.*, Phys. Plasmas **7**, 2578 (2000).

⁹F. H. Séguin, C. K. Li, J. A. Frenje *et al.*, Phys. Plasmas **9**, 2725 (2002).

¹⁰S. Skupsky and R. S. Craxton, Phys. Plasmas **6**, 2157 (1999).

¹¹C. K. Li, F. H. Séguin, D. G. Hicks *et al.*, Phys. Plasmas **8**, 4902 (2001).

¹²D. D. Meyerhofer, J. A. Delettrez, R. Epstein *et al.*, Phys. Plasmas **8**, 2251 (2001).

¹³C. K. Li, F. H. Séguin, J. A. Frenje *et al.*, "Effects of fuel-shell mix upon direct-drive, spherical implosions on OMEGA," Phys. Rev. Lett. (submitted).

¹⁴F. J. Marshall, J. A. Delettrez, R. L. Keck, J. H. Kelly, P. B. Radha, and L. J. Waxer, Bull. Am. Phys. Soc. **46**, 179 (2001).

¹⁵D. G. Hicks, C. K. Li, R. D. Petrasso, F. H. Séguin, B. E. Burke, J. P. Knauer, S. Cremer, R. L. Kremens, M. D. Cable, and T. W. Phillips, Rev. Sci. Instrum. **68**, 589 (1997).

¹⁶F. H. Séguin, J. A. Frenje, C. K. Li *et al.*, "Spectrometry of charged particles from inertial-confinement-fusion plasmas," Rev. Sci. Instrum. (to be published).

¹⁷C. K. Li and R. D. Petrasso, Phys. Rev. Lett. **70**, 3059 (1993).

¹⁸D. G. Hicks, C. K. Li, F. H. Séguin *et al.*, Phys. Plasmas **7**, 5106 (2000).

¹⁹If $\Theta_l \ll 2\theta_s (l \gg \pi/\theta_s)$, no variations in either energy or fluence would be measured, because at any detector angle ϕ the protons from multiple cycles of ρR fluctuations would be averaged together. If $\Theta_l \sim 2\theta_s (l \sim \pi/\theta_s)$, variations in both energy and fluence would be detected. If $\Theta_l \gg 2\theta_s (l \ll \pi/\theta_s)$, each detector would sample a portion of the capsule that was small compared to the wavelength of the ρR fluctuations, and therefore locally uniform. Angular variations in energy would be detectable, because all protons at a given detector would have the energy loss characteristic of the corresponding local $\rho R(\phi)$. Angular variations in fluence would not be measured; for each detector the angular size of the capsule region sampled is proportional to $\theta_s(\phi)$, and this precisely compensates for the fact that the number of protons intercepted per unit ϕ in the capsule is proportional to $1/\theta_s(\phi)$. In the particular limit $l=0$, where the capsule remains spherical and ρR is modified by the same factor $[1+A]$ at all ϕ , any change in A will result in a corresponding change in ΔE for all detectors but can have no impact on measured fluences (assuming that the particle production rate in the fuel is unchanged).

²⁰J. F. Ziegler, J. P. Biersack, and U. Littmark, *The Stopping and Range of Ions in Solids, Vol. 1* (Pergamon, New York, 1985), and SRIM, a code for calculations of the Stopping and Range of Ions in Matter, Jan. 1, 2000, Version 0.05. (J. F. Ziegler and J. P. Biersack).

²¹C. Stoeckl, C. Chiritescu, J. A. Delettrez *et al.*, Phys. Plasmas **9**, 2195 (2002).

²²R. D. Petrasso, C. K. Li, F. H. Séguin *et al.*, Bull. Am. Phys. Soc. **46**, 105 (2001).

²³H. Azechi, M. D. Cable, and R. O. Stapf, Laser Part. Beams **9**, 119 (1991).

²⁴The theoretical possibility of magnetic fields modifying local particle fluences was discussed in Ref. 5.